

Stabilizing fractional Chern insulators via exchange interaction in moiré systems

Xiaoyang Shen,^{1,*} Chonghao Wang,^{1,*} Ruiping Guo,^{1,2,*} Zhiming Xu,¹ Wenhui Duan,^{1,2,3,4,†} and Yong Xu^{1,3,5,‡}

¹*State Key Laboratory of Low Dimensional Quantum Physics and
Department of Physics, Tsinghua University, Beijing, 100084, China*

²*Institute for Advanced Study, Tsinghua University, Beijing 100084, China*

³*Frontier Science Center for Quantum Information, Beijing, China*

⁴*Beijing Academy of Quantum Information Sciences, Beijing 100193, China*

⁵*RIKEN Center for Emergent Matter Science (CEMS), Wako, Saitama 351-0198, Japan*

(Dated: May 22, 2024)

Recent experimental discovery of fractional Chern insulator in moiré Chern band in twisted transition metal dichalcogenide homobilayers has sparked intensive interest in exploring the ways of engineering band topology and correlated states in moiré systems. In this letter, we demonstrate that, with an additional exchange interaction induced by proximity effect, the topology and bandwidth of the moiré minibands of twisted MoTe₂ homobilayers can be easily tuned. Fractional Chern insulators at $-2/3$ filling are found to appear at enlarged twist angles over a large range of twist angles with enhanced many-body gaps. We further discover a topological phase transition between the fractional Chern insulator, quantum anomalous Hall crystal, and charge density wave. Our results shed light on the interplay between topology and correlation physics.

Introductions.— Moiré materials based on multilayer van de Waals materials have recently become a burgeoning area with intensive study. The dominance of many-body interaction over kinetic energy plays a pivotal role in the emergence of the remarkable exotic phases, such as correlated insulators, superconductivity, and generalized Wigner crystals [1–6]. Among the strongly correlated electron states, the investigation of fractional Chern insulators (FCIs) holds a broad appeal due to its novel nature and potential to serve as the possible platform for quantum computation [7, 8]. Amounts of theoretical works [9–13] have predicted that FCI finds its manifestation in moiré materials such as twisted bilayer graphene (TBG) and twisted bilayer transition metal dichalcogenide (TMD), which has later been witnessed in the experiments [5, 14–17]. However, the presence of FCIs usually requires strong conditions on both dispersion and interaction [18–23]. For instance, in reminiscence of the Landau levels in the two-dimensional electron gases, the partially filled moiré band should be nearly flat and topological. Besides, the quantum geometric characterized by the Fubini-Study metric should also be flat. The interaction should be strong enough to induce the many-body gap between the degenerated ground states and the excited states. As a result, the existence of FCIs is usually fragile against fluctuations and hence it is not easy to reach in both theoretical and experimental attempts [5, 14, 24].

Searching for the feasibility of stabilizing such an exotic phase would be intriguing and significant. From the perspective of band structure, the flatness comes from manipulating the spatially modulated moiré potential. Such modulation also emerges in the magnetic materials with moiré structures [25, 26]. This indicates that the proximity exchange interaction may serve as a potential ingredient in tuning the moiré potential and further ma-

nipulating and stabilizing the novel phase in the moiré material [25, 27].

In this Letter, we demonstrate that the proximity magnetic exchange interaction serves as an effective way to stabilize the FCIs and manipulate the correlated phases in moiré materials. Taking the twisted bilayer MoTe₂ as an example, under the proximity exchange interaction, the flat band is supported in a large range of twist angles, and the band topology exhibits a rich structure with respect to the exchange strength and the twist angle. Utilizing the exact diagonalization (ED), we find the existence of FCI in a wide range of twist angles, together with a prominent enhancement of the many-body gap. We further investigate the competition between FCIs and the charge density waves (CDWs) at $-2/3$ filling under the exchange interaction. We report exotic exchange-interaction-induced topological phase transitions between the FCI, a charge-ordered phase with intrinsically topological nature, which is recently dubbed as *quantum anomalous Hall crystal* (QAHC) [28–30] and topologically trivial CDW [31–33].

Continuum model.— The starting point is the single particle moiré Hamiltonian of the twisted bilayer MoTe₂ with the proximity exchange interaction [24, 34–36].

$$\mathcal{H}(\mathbf{r}) = \mathcal{H}_0(\mathbf{r}) + \mathcal{H}_{\text{ex}}(\mathbf{r}) \quad (1)$$

Without exchange interaction, \mathcal{H}_0 is the Hamiltonian without the exchange interaction and can be split into two time-reversal counterparts $\mathcal{H}_{\tau=\pm 1}$ with opposite valleys and spins.

$$\mathcal{H}_{\tau}(\mathbf{r}) = \begin{pmatrix} -\frac{\hbar^2(\mathbf{k}-\tau\boldsymbol{\kappa}_+)^2}{2m^*} + \Delta_{\text{b}}(\mathbf{r}) & \Delta_{\text{T}}(\mathbf{r}) \\ \Delta_{\text{T}}^{\dagger}(\mathbf{r}) & -\frac{\hbar^2(\mathbf{k}-\tau\boldsymbol{\kappa}_-)^2}{2m^*} + \Delta_{\text{t}}(\mathbf{r}) \end{pmatrix}, \quad (2)$$

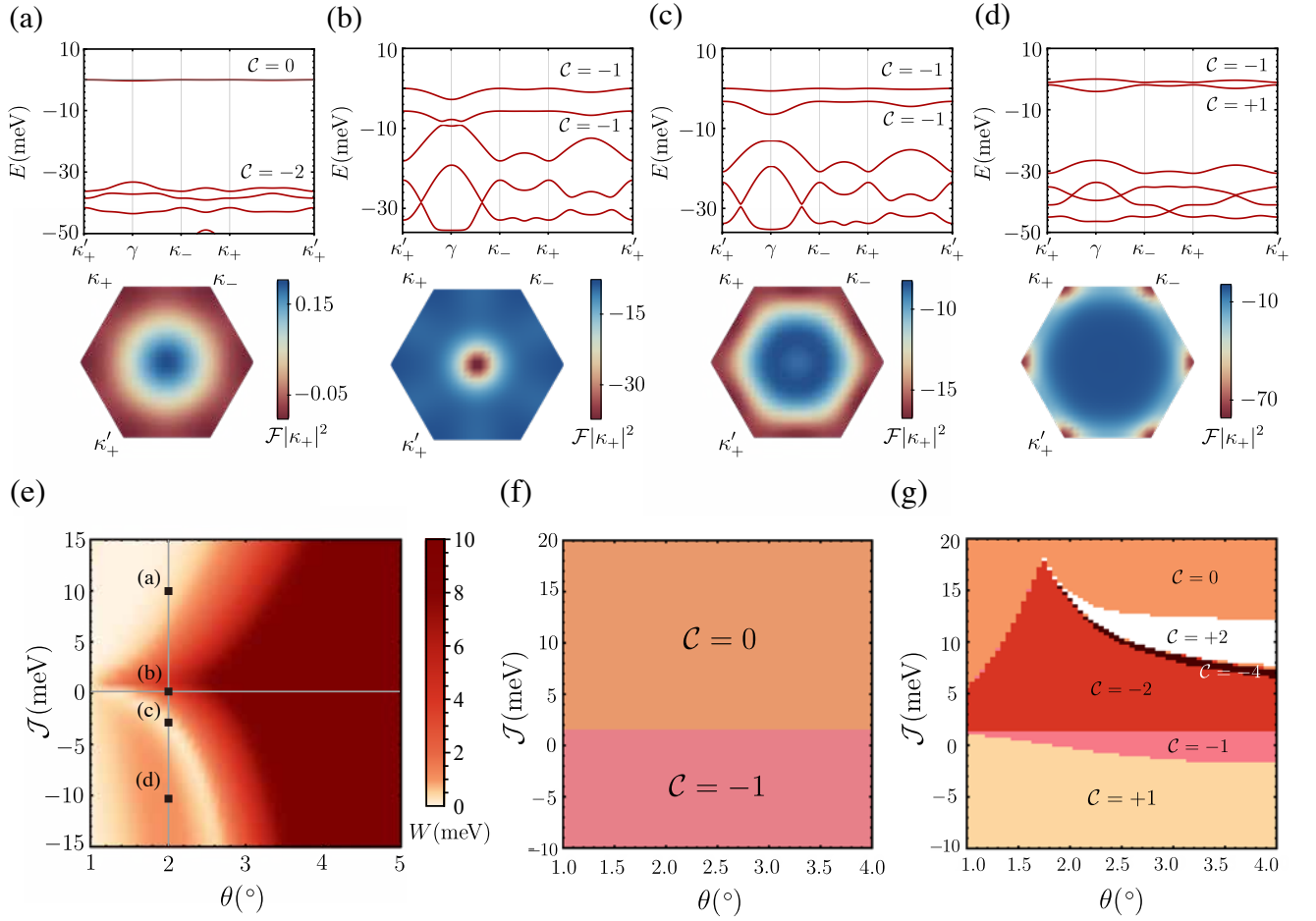


FIG. 1. (a)-(d) Band structure and the Berry curvature \mathcal{F} at $\theta = 2^\circ$, $\mathcal{J} = 10, 0, -2, 10$ meV, respectively. (e) Bandwidth W of the first valence band as a function of twist angle θ and exchange interaction strength \mathcal{J} . (f) Chern number \mathcal{C} of the first valence band as a function of θ and \mathcal{J} . (g) Chern number \mathcal{C} of the second valence band as a function of θ and \mathcal{J} .

where

$$\begin{aligned} \Delta_{t,b}(\mathbf{r}) &= 2V \sum_{j=1,3,5} \cos(\mathbf{g}_j \cdot \mathbf{r} + \ell\psi) \\ \Delta_T(\mathbf{r}) &= w(1 + e^{-i\tau\mathbf{g}_2 \cdot \mathbf{r}} + e^{-i\tau\mathbf{g}_3 \cdot \mathbf{r}}) \end{aligned} \quad (3)$$

$\Delta_{t,b}(\mathbf{r})$ is the intralayer moiré potential, $\ell = 1$ for the top layer and -1 bottom layer, and V, ψ capture the amplitude and shape of the potential. $\Delta_T(\mathbf{r})$ is the inter-layer tunneling terms, and w characterizes the amplitude of the tunneling. m^* is the effective mass. In our numerical calculations, we take the parameters from fitting the first-principles calculation as in [35]: $V = 8.0$ meV, $\psi = -89.6^\circ$ and $w = -8.5$ meV. $\mathbf{g}_j, j = 1, \dots, 6$ are the reciprocal lattice vectors.

\mathcal{H}_\pm are related to each other via the time-reversal symmetry (TRS) operator \mathcal{T} . The exchange interaction $J\hat{S}(\mathbf{r}) \cdot \hat{\sigma}$ acts on the spin which is locked to valley. Due to the dominated splitting from spin-orbit coupling (SOC) ~ 164 meV, the off-diagonal element $J\hat{S}_x(\mathbf{r}) \pm iJ\hat{S}_y(\mathbf{r})$ can be neglected. The position-dependent proximity ex-

change interaction from the proximal magnet for each τ now is

$$\mathcal{H}_{ex,\tau}(\mathbf{r}) = \begin{pmatrix} \tau J_b S_z(\mathbf{r}) & 0 \\ 0 & \tau J_t S_z(\mathbf{r}) \end{pmatrix}, \quad (4)$$

$J_{b(t)}$ is the strength of the exchange interaction for the bottom(top) layer and $S_z(\mathbf{r})$ is the position-dependent spin texture varying periodically in real space. The spin texture from the proximal magnet serves as the external source to tune the moiré potential. Several proposals for moiré magnet with highly-tunable period and giant exchange strength have been proposed and analyzed [25, 26, 37]. Without loss of generality, the simplest C_6 symmetric spin texture commensurate with the underlying moiré lattice, together with the layer-independent interaction strength $J_{b,t} = J$ are assumed in the following. The exchange interaction strength from the averaged magnetization in the moiré unit cell (MUC) and the first Fourier component is denoted as \mathcal{J}_0 and \mathcal{J}

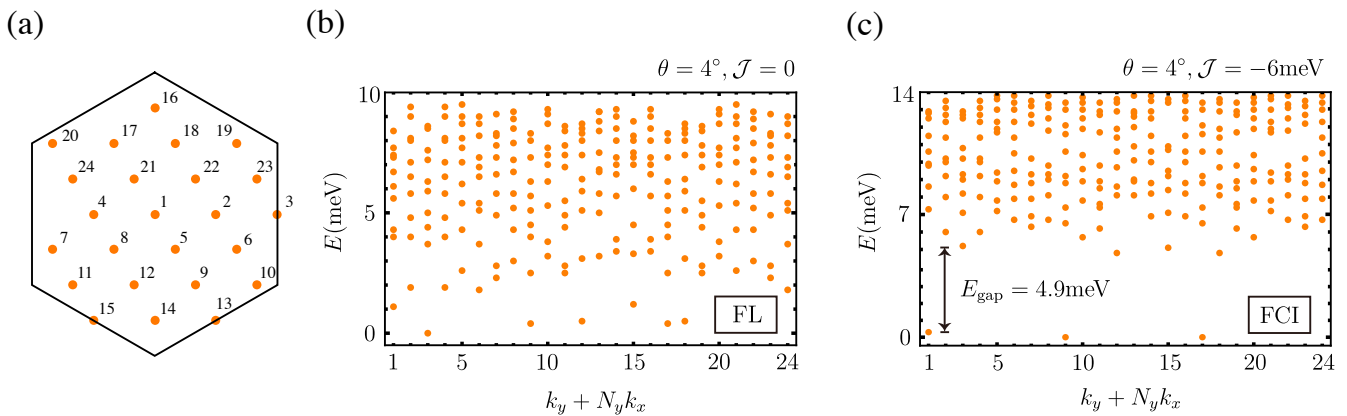


FIG. 2. (a) Distribution of 4×6 k-point grid in ED. (b)(c) Many-body spectrum distribution as functions of center-of-mass momentum at $\theta = 4^\circ$ with $\mathcal{J} = 0$ and $\mathcal{J} = -6$ meV, respectively. The Fermi liquid (FL) for vanishing exchange interaction strength $\mathcal{J} = 0$ and FCI with a sizable many-body gap (~ 4.9 meV) for $\mathcal{J} = -6$ meV are observed.

$$\mathcal{J}_0 = J \int_{\text{MUC}} d^2 \mathbf{r} S_z(\mathbf{r}), \quad \mathcal{J} = J \int_{\text{MUC}} d^2 \mathbf{r} e^{i \mathbf{g}_i \cdot \mathbf{r}} S_z(\mathbf{r}). \quad (5)$$

and short-wavelength components are neglected. The exchange interaction breaks \mathcal{T} , lifting the degeneracy between different valleys, rendering the system a valley-polarized Chern insulator at integer filling.

Band structure and topology.— The constant Zeeman energy \mathcal{J}_0 does not change the band structure and topology and only shifts the relative position of valence bands from different valleys. We now fix \mathcal{J}_0 to a large value to guarantee the topmost valence bands are from a single copy of valley. \mathcal{J} plays a central role in tuning the bandwidth and endowing a rich structure of band topology, as illustrated in Fig.1. Fig.1 (e) illustrates the bandwidth as the function of θ and \mathcal{J} . The band is flattened in the presence of exchange interaction, and the flat band exists in a wide range of twist angles. The magic angle where the ideal flat band emerges increases with the absolute value of \mathcal{J} .

The extensiveness of the nearly zero bandwidth implies that the exchange interaction may help promote the robustness of the flat bands. Fig.1 (f)(g) exhibits the Chern numbers of the first and second valence bands. Fig.1 (f) depicts a topological phase transition induced by the exchange interaction at the critical value of 1.56 meV. When \mathcal{J} exceeds 1.56 meV, the Chern number of the second band also changes from $\mathcal{C} = -1$ to $\mathcal{C} = -2$ which is attributed to the gap closing at γ point between the first and the second valence band. The Chern number of the first valence band keeps vanishing and the bandgap increases with \mathcal{J} . However, the second and the third bands get closer and interact with each other with frequent band inversions, leading to a rich topological phase diagram in Fig.1 (g).

To gain a deeper view of the topology and the origin of the flat band, we track the band structure and Berry

curvature of the first valence band along \mathcal{J} with fixed angle $\theta = 2^\circ$. When $\mathcal{J} = 10$ meV as shown in Fig.1 (a), the first valence band is perfectly flat and topologically trivial, serving as a potential candidate for hosting the stripe phase. As \mathcal{J} decreases, the topological phase transition happens, and the Berry curvature at $\mathcal{J} = 0$ is mainly concentrated at γ , as shown in Fig.1 (b). When \mathcal{J} is negative, as shown in Fig.1 (b-d), the Berry curvature starts to transfer from γ to κ points with the Chern number $\mathcal{C} = -1$ fixed. Hence there exists an intermediate point with uniformly distributed Berry curvature and flat band structure.

It is worth noting that several sets of parameters (V, w, ψ) have been proposed by fitting from different density functional theory results [24, 38, 39]. In practice, we test for different sets of parameters and get similar results, demonstrating the robustness and reliability of our conclusions.

Stabilize the Fractional Chern insulator.— Having established the existence of isolated flat Chern bands appearing over a wide range of twist angles, we investigate whether FCIs can be stabilized by proximity-induced exchange interaction. We solve the many-body Hamiltonian using the exact diagonalization methodology. The Coulomb interaction is

$$\mathcal{H}_{\text{int}} = \frac{1}{2A} \sum_{\mathbf{k}, \mathbf{k}', \mathbf{q}} \sum_{\text{BZ}} \lambda_{n_1, n_2, n_3, n_4}^{\mathbf{k}, \mathbf{k}', \mathbf{q}} c_{n_1, \mathbf{k} + \mathbf{q}}^\dagger c_{n_2, \mathbf{k}' - \mathbf{q}}^\dagger c_{n_3, \mathbf{k}'} c_{n_4, \mathbf{k}}, \quad (6)$$

where $c_{n, \mathbf{k}}^\dagger$ ($c_{n, \mathbf{k}}$) is the creation(annihilation) operator of the Bloch state, A is the total area of the system, and n_1, n_2, n_3, n_4 are band indices. The form factor $\lambda_{n_1, n_2, n_3, n_4}^{\mathbf{k}, \mathbf{k}', \mathbf{q}}$ is given by:

$$\lambda_{n_1, n_2, n_3, n_4}^{\mathbf{k}, \mathbf{k}', \mathbf{q}} = \sum_{\mathbf{G}} V(\mathbf{q} + \mathbf{G}) \langle u_{n_1, \mathbf{k} + \mathbf{q} + \mathbf{G}} | u_{n_4, \mathbf{k}} \rangle \times \langle u_{n_2, \mathbf{k}' - \mathbf{q} - \mathbf{G}} | u_{n_3, \mathbf{k}'} \rangle. \quad (7)$$

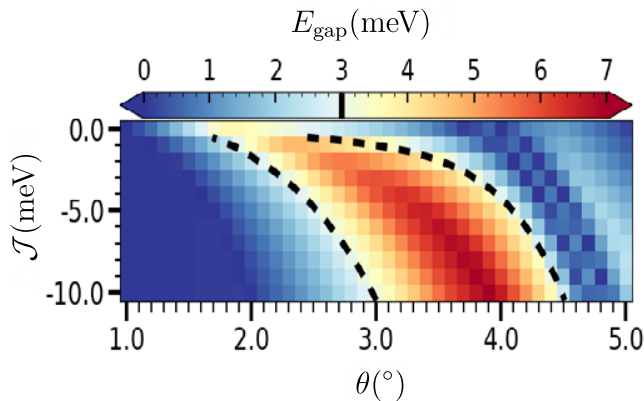


FIG. 3. Many-body gap E_{gap} as functions of \mathcal{J} and θ . $E_{\text{gap}} \equiv E_4 - E_3$ where E_i is the many-body eigenstate of i^{th} lowest energy as a function of twist angle θ as well as \mathcal{J} . The dashed line corresponds to $E_{\text{gap}} = 3$ meV. The ED calculation is carried out with 4×6 unit cells; the gate-distance is chosen as $d = 300$ Å and the relative dielectric constant ϵ is 6.

where $|u_{n,\mathbf{k}}\rangle$ is the periodic part of the Bloch state, $V(\mathbf{q}) = e^2 \tanh(|\mathbf{q}|d)/2\epsilon_0\epsilon|\mathbf{q}|$ is the double-gated screened Coulomb potential with gate distance d , and ϵ is the dielectric constant [24]. Since the exchange interaction explicitly breaks TRS, we are permitted to project the interaction onto the topmost valence band from a single valley. From the perspective of symmetry, TRS-breaking phases such as the Chern insulator, ferromagnet, and the FCI are preferred. In the following, the calculation is performed with 4×6 mesh of grids in the first Brillouin zone. The gate distance is chosen to be 30 nm and the dielectric constant is set to be 6.

To investigate the existence of FCI, we start with some representative samplings. Two samplings with $\mathcal{J} = 0$ and $\mathcal{J} = -6$ meV at fixed angle $\theta = 4^\circ$ are first analyzed. In the absence of exchange interaction, from Fig. 2 (b), there is neither three-fold-degeneracy of the ground states nor a sizable gap, which can be attributed to the dispersive band structure with Berry curvature mainly concentrating at γ point. Thus the ground state is the Fermi liquid (FL) for small \mathcal{J} . However, as we increase the exchange interaction strength, the band is flattened and FCI starts to emerge as shown in Fig. 2 (c) with a many-body gap $E_{\text{gap}} = 4.9$ meV. The many-body gap is defined as the energy difference between the first excited states and the three-fold-degenerate ground states. The three-fold-degenerate ground states respect the generalized Pauli principle and change with the period of $3 \times 2\pi$ under flux insertion.

The many-body gap E_{gap} is further evaluated by sweeping twist angle θ and the strength of the exchange interaction \mathcal{J} , as shown in Fig. 3. Remarkably, the many-body gap is prominently enhanced with the increasing strength of the exchange interaction \mathcal{J} . The

range of the twist angle with the sizable gap grows with the exchange interaction strength, implying that under the exchange interaction, the emergence of FCI may be robust to the twist angle. The dashed line in Fig. 3 corresponds to $E_{\text{gap}} = 3$ meV, at which the notable enhancing effect can be observed. The above analysis clearly demonstrates that FCIs can be stabilized by proximity-induced exchange interaction.

Exchange interaction driven phase transition.— In the previous section, we report a topological transition in the flat band from $\mathcal{C} = 0$ to $\mathcal{C} = -1$ driven by the exchange interaction and a stabilized FCI when $\mathcal{C} = -1$. The flat band with zero Chern number naturally serves as a platform for hosting the stripe phase, such as the generalized Wigner crystal and CDW. It would be intriguing to unravel the intertwining between the CDW and FCI when the topologically trivial band is endowed with a non-vanishing Chern number.

In the following, we perform an exact diagonalization calculation and track the ground states along with \mathcal{J} at a fixed twist angle. The exact diagonalization is carried out on the grid of 12 k-points in BZ in the lower panel of Fig. 4. These 12 k-points maintain the rotation symmetry, including the high symmetry points γ , κ , κ' , and M. The dielectric constant ϵ is set to be 6 and the twisted angle is fixed to be 4° . For each \mathcal{J} , we assemble the states with different center-of-mass momentum and track the first several states with the lowest energy. When \mathcal{J} ranges from -10 to -1 meV, the ground state exhibits three-fold degeneracy with a sizable many-body gap increasing with the absolute value of \mathcal{J} . As illustrated in the previous result, the ground state obeys the generalized Pauli principle [19, 40] and the phase is identified as the FCI. As \mathcal{J} approaches -1 meV, the energy gap between the third state and the fourth state decreases, and the level crossing happens at $\mathcal{J} = -1$ meV, implying some subtle change of topological order of the phase. When \mathcal{J} exceeds 1.56 meV, the topological phase transition from $\mathcal{C} = -1$ to 0 takes place, rendering a discontinuous redistribution of the ground state. When \mathcal{J} is positive away from 0, an enormous charge gap ~ 10 meV emerges and we find a three-fold degeneracy at the κ, κ' and γ points independent of the choice of the grids. Together with the vanishing Chern number, we identify the phase as the topologically trivial $\sqrt{3} \times \sqrt{3}$ CDW.

To further unravel the topological order of these phases, we evaluate the many-body Chern number as a probe. The many-body Chern number is defined as the integral of Berry curvature over the phase space of the twist boundary condition [41, 42].

$$C_{\text{MB}} = \frac{i}{2\pi} \iint_0^{2\pi} d\theta_x d\theta_y \left(\left\langle \frac{\partial \psi}{\partial \theta_y} \middle| \frac{\partial \psi}{\partial \theta_x} \right\rangle - \text{c.c.} \right) \quad (8)$$

where ψ is the many-body wave function and θ_x and θ_y are the angles of twist boundary condition along two lattice vectors. We perform the numerical evaluation of

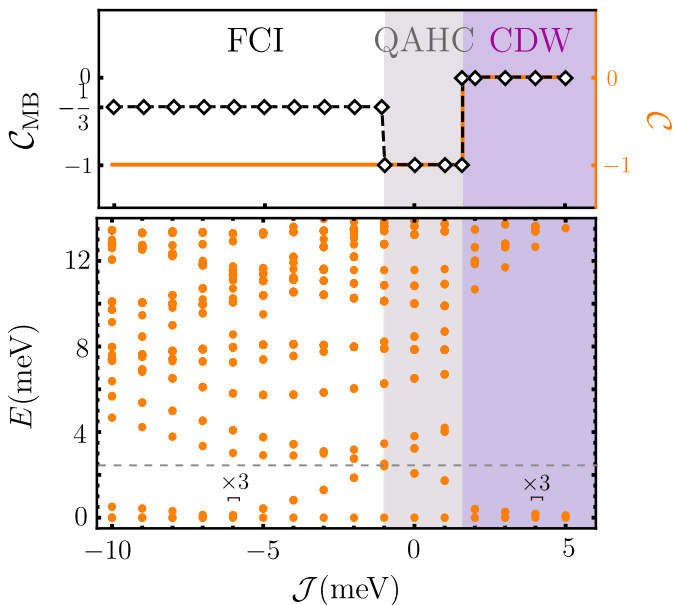


FIG. 4. The upper panel is the many-body Chern number C_{MB} (black) and Chern number C (orange) changing with exchange interaction. The lower panel is the spectrum changing with exchange interaction strength at $\theta = 4^\circ$. Two panels share the same horizontal axis.

Berry curvature under a 10×10 discretization of phase space. The Chern number and many-body Chern number are provided in the upper panel of Fig.(4). We demonstrate two topological phase transitions as changing \mathcal{J} . The first phase transition takes place when $\mathcal{J} = -1\text{meV}$ between the $\nu = -\frac{2}{3}$ FCI and the QAH with Hall conductance $\sigma_H = -1$ even when at the fractional filling. The latter phase originates from the interplay between the CDW and FCI and is recently dubbed the quantum anomalous Hall crystal (QAHC). The QAHC is a sort of topological charge density wave, as the phase resides at a topologically nontrivial band and exhibits the $\sqrt{3} \times \sqrt{3}$ charge order. A way of interpreting the phase is that the emergence of $\sqrt{3} \times \sqrt{3}$ charge order spontaneously breaks the transversal symmetry, enlarging the unit cell 3 times, hence at $-\frac{2}{3}$ filling the mini-band is totally filled, leaving the integer Hall conductance $\sigma_H = -1$. The second topological phase transition between the QAHC and CDW is induced by the single-particle topology, which changes the Bloch wavefunctions discontinuously at gap closing. Observation of the Hall conductance varies from $\sigma_H = -1$ to $\sigma_H = 0$ is a typical signal of the phase transition.

Conclusions. — In this Letter, we study the twisted bilayer TMD in the presence of moiré proximity exchange interaction. We find that the exchange interaction assists in flattening the band structure. The wide-ranged existence of the flat band and the explicit breaking of TRS provide a platform for extensively hosting the FCIs. By carrying out the ED, we confirm the stabilizing of FCIs

by observing a prominently enhanced many-body gap. Besides, the band topology also exhibits a rich structure driven by the exchange interaction. We report an exotic quantum phase transition between CDW, QAHC, and FCI induced by exchange interaction. In summary, we believe that our work not only leads to concrete support that proximity exchange interaction serves as an effective and practical way of manipulating the band structure and correlated electronic phase, but also sheds light on the profound interplay between topology, symmetry, and correlation.

* These authors contributed equally to the work.

† duanw@tsinghua.edu.cn

‡ yongxu@mail.tsinghua.edu.cn;

- [1] Yuan Cao, Valla Fatemi, Shiang Fang, Kenji Watanabe, Takashi Taniguchi, Efthimios Kaxiras, and Pablo Jarillo-Herrero. Unconventional superconductivity in magic-angle graphene superlattices. *Nature*, 556(7699):43–50, 2018.
- [2] Yuan Cao, Valla Fatemi, Ahmet Demir, Shiang Fang, Spencer L Tomarken, Jason Y Luo, Javier D Sanchez-Yamagishi, Kenji Watanabe, Takashi Taniguchi, Efthimios Kaxiras, et al. Correlated insulator behaviour at half-filling in magic-angle graphene superlattices. *Nature*, 556(7699):80–84, 2018.
- [3] Hongyuan Li, Ziyu Xiang, Emma Regan, Wenyu Zhao, Renee Sailus, Rounak Banerjee, Takashi Taniguchi, Kenji Watanabe, Sefaattin Tongay, Alex Zettl, et al. Mapping charge excitations in generalized wigner crystals. *Nature nanotechnology*, pages 1–6, 2024.
- [4] Emma C Regan, Danqing Wang, Chenhao Jin, M Iqbal Bakti Utama, Beini Gao, Xin Wei, Sihan Zhao, Wenyu Zhao, Zuo Cheng Zhang, Kentaro Yumigeta, et al. Mott and generalized wigner crystal states in $w\text{se}_2/w\text{s}_2$ moiré superlattices. *Nature*, 579(7799):359–363, 2020.
- [5] Yonglong Xie, Andrew T Pierce, Jeong Min Park, Daniel E Parker, Eslam Khalaf, Patrick Ledwith, Yuan Cao, Seung Hwan Lee, Shaowen Chen, Patrick R Forrester, et al. Fractional chern insulators in magic-angle twisted bilayer graphene. *Nature*, 600(7889):439–443, 2021.
- [6] Yonglong Xie, Biao Lian, Berthold Jäck, Xiaomeng Liu, Cheng-Li Chiu, Kenji Watanabe, Takashi Taniguchi, B. Andrei Bernevig, and Ali Yazdani. Spectroscopic signatures of many-body correlations in magic-angle twisted bilayer graphene. *Nature*, 572(7767):101–105, July 2019.
- [7] Chetan Nayak, Steven H Simon, Ady Stern, Michael Freedman, and Sankar Das Sarma. Non-abelian anyons and topological quantum computation. *Reviews of Modern Physics*, 80(3):1083–1159, 2008.
- [8] A Yu Kitaev. Fault-tolerant quantum computation by anyons. *Annals of physics*, 303(1):2–30, 2003.
- [9] Heqiu Li, Umesh Kumar, Kai Sun, and Shi-Zeng Lin. Spontaneous fractional Chern insulators in transition metal dichalcogenide moiré superlattices. *Physical Review Research*, 3(3):L032070, September 2021.
- [10] Trithap Devakul, Valentin Crépel, Yang Zhang, and Liang Fu. Magic in twisted transition metal dichalco-

- genide bilayers. *Nature Communications*, 12:6730, November 2021.
- [11] Ahmed Abouelkomsan, Zhao Liu, and Emil J. Bergholtz. Particle-hole duality, emergent fermi liquids, and fractional chern insulators in moiré flatbands. *Phys. Rev. Lett.*, 124:106803, Mar 2020.
- [12] Cécile Repellin and T. Senthil. Chern bands of twisted bilayer graphene: Fractional chern insulators and spin phase transition. *Phys. Rev. Res.*, 2:023238, May 2020.
- [13] Patrick Wilhelm, Thomas C. Lang, and Andreas M. Läuchli. Interplay of fractional chern insulator and charge density wave phases in twisted bilayer graphene. *Phys. Rev. B*, 103:125406, Mar 2021.
- [14] Jiaqi Cai, Eric Anderson, Chong Wang, Xiaowei Zhang, Xiaoyu Liu, William Holtzmann, Yinong Zhang, Fengren Fan, Takashi Taniguchi, Kenji Watanabe, Ying Ran, Ting Cao, Liang Fu, Di Xiao, Wang Yao, and Xiaodong Xu. Signatures of fractional quantum anomalous hall states in twisted mote2. *Nature*, 622(7981):63–68, Oct 2023.
- [15] Heonjoon Park, Jiaqi Cai, Eric Anderson, Yinong Zhang, Jiayi Zhu, Xiaoyu Liu, Chong Wang, William Holtzmann, Chaowei Hu, Zhaoyu Liu, Takashi Taniguchi, Kenji Watanabe, Jiun-Haw Chu, Ting Cao, Liang Fu, Wang Yao, Cui-Zu Chang, David Cobden, Di Xiao, and Xiaodong Xu. Observation of fractionally quantized anomalous hall effect. *Nature*, 622(7981):74–79, Oct 2023.
- [16] Fan Xu, Zheng Sun, Tongtong Jia, Chang Liu, Cheng Xu, Chushan Li, Yu Gu, Kenji Watanabe, Takashi Taniguchi, Bingbing Tong, Jinfeng Jia, Zhiwen Shi, Shengwei Jiang, Yang Zhang, Xiaoxue Liu, and Tingxin Li. Observation of integer and fractional quantum anomalous hall effects in twisted bilayer mote₂. *Phys. Rev. X*, 13:031037, Sep 2023.
- [17] Zhengguang Lu, Tonghang Han, Yuxuan Yao, Aidan P. Reddy, Jixiang Yang, Junseok Seo, Kenji Watanabe, Takashi Taniguchi, Liang Fu, and Long Ju. Fractional quantum anomalous hall effect in multilayer graphene. *Nature*, 626(8000):759–764, Feb 2024.
- [18] Rahul Roy. Band geometry of fractional topological insulators. *Phys. Rev. B*, 90:165139, Oct 2014.
- [19] Nicolas Regnault and B Andrei Bernevig. Fractional chern insulator. *Physical Review X*, 1(2):021014, 2011.
- [20] Xiao-Liang Qi. Generic wave-function description of fractional quantum anomalous hall states and fractional topological insulators. *Phys. Rev. Lett.*, 107:126803, Sep 2011.
- [21] T. S. Jackson, Gunnar Möller, and Rahul Roy. Geometric stability of topological lattice phases. *Nature Communications*, 6(1), November 2015.
- [22] Siddharth A. Parameswaran, Rahul Roy, and Shivaji L. Sondhi. Fractional quantum hall physics in topological flat bands. *Comptes Rendus. Physique*, 14(9–10):816–839, June 2013.
- [23] Jie Wang, Jennifer Cano, Andrew J. Millis, Zhao Liu, and Bo Yang. Exact landau level description of geometry and interaction in a flatband. *Phys. Rev. Lett.*, 127:246403, Dec 2021.
- [24] Chong Wang, Xiao-Wei Zhang, Xiaoyu Liu, Yuchi He, Xiaodong Xu, Ying Ran, Ting Cao, and Di Xiao. Fractional chern insulator in twisted bilayer mote 2. *Physical Review Letters*, 132(3):036501, 2024.
- [25] Nisarga Paul, Yang Zhang, and Liang Fu. Giant proximity exchange and flat chern band in 2d magnet-semiconductor heterostructures. *Science Advances*, 9(8):eabn1401, 2023.
- [26] Qingjun Tong, Fei Liu, Jiang Xiao, and Wang Yao. Skyrmions in the Moiré of van der Waals 2D Magnets. *Nano Letters*, 18(11):7194–7199, November 2018.
- [27] Nicolás Morales-Durán, Nemin Wei, Jingtian Shi, and Allan H. MacDonald. Magic angles and fractional chern insulators in twisted homobilayer transition metal dichalcogenides. *Phys. Rev. Lett.*, 132:096602, Mar 2024.
- [28] DN Sheng, AP Reddy, A Abouelkomsan, EJ Bergholtz, and L Fu. Quantum anomalous hall crystal at fractional filling of moiré superlattices. *arXiv preprint arXiv:2402.17832*, 2024.
- [29] Xue-Yang Song, Chao-Ming Jian, Liang Fu, and Cenke Xu. Intertwined fractional quantum anomalous hall states and charge density waves. *Physical Review B*, 109(11):115116, 2024.
- [30] Xue-Yang Song, Ya-Hui Zhang, and T. Senthil. Phase transitions out of quantum Hall states in moiré materials. *Phys. Rev. B*, 109(8):085143, February 2024.
- [31] Aidan P Reddy and Liang Fu. Toward a global phase diagram of the fractional quantum anomalous hall effect. *Physical Review B*, 108(24):245159, 2023.
- [32] Prakash Sharma, Yang Peng, and D. N. Sheng. Topological quantum phase transitions driven by displacement fields in the twisted mote2 bilayers, 2024.
- [33] Peng-Sheng Hu, Yi-Han Zhou, and Zhao Liu. Floquet fractional chern insulators and competing phases in twisted bilayer graphene. *SciPost Physics*, 15(4), October 2023.
- [34] Rafi Bistritzer and Allan H. MacDonald. Moiré bands in twisted double-layer graphene. *Proceedings of the National Academy of Sciences*, 108(30):12233–12237, July 2011.
- [35] Fengcheng Wu, Timothy Lovorn, Emanuel Tutuc, Ivar Martin, and AH MacDonald. Topological insulators in twisted transition metal dichalcogenide homobilayers. *Physical review letters*, 122(8):086402, 2019.
- [36] Yujin Jia, Jiabin Yu, Jiaxuan Liu, Jonah Herzog-Arbeitman, Ziyue Qi, Hanqi Pi, Nicolas Regnault, Hongming Weng, B. Andrei Bernevig, and Quansheng Wu. Moiré fractional Chern insulators. I. First-principles calculations and continuum models of twisted bilayer MoTe₂. *Phys. Rev. B*, 109(20):205121, May 2024.
- [37] Hongchao Xie, Xiangpeng Luo, Zhipeng Ye, Zeliang Sun, Gaihua Ye, Suk Hyun Sung, Haiwen Ge, Shaohua Yan, Yang Fu, Shangjie Tian, Hechang Lei, Kai Sun, Robert Hovden, Rui He, and Liuyan Zhao. Evidence of non-collinear spin texture in magnetic moiré superlattices. *Nature Physics*, 19(8):1150–1155, August 2023.
- [38] Aidan P Reddy, Faisal Alsallom, Yang Zhang, Trithep Devakul, and Liang Fu. Fractional quantum anomalous hall states in twisted bilayer mote 2 and wse 2. *Physical Review B*, 108(8):085117, 2023.
- [39] Cheng Xu, Jiangxu Li, Yong Xu, Zhen Bi, and Yang Zhang. Maximally localized wannier functions, interaction models, and fractional quantum anomalous hall effect in twisted bilayer mote2. *Proceedings of the National Academy of Sciences*, 121(8):e2316749121, 2024.
- [40] EJ Bergholtz and Anders Karlhede. Quantum hall system in tao-thouless limit. *Physical Review B*, 77(15):155308, 2008.
- [41] Koji Kudo, Haruki Watanabe, Toshikaze Kariyado, and

- Yasuhiro Hatsugai. Many-body chern number without integration. *Physical review letters*, 122(14):146601, 2019.
- [42] Qian Niu, Ds J Thouless, and Yong-Shi Wu. Quantized hall conductance as a topological invariant. *Physical Review B*, 31(6):3372, 1985.